Surface enrichment of biomimetic apatites with biologically-active ions Mg^{2+} and Sr^{2+}: A preamble to the activation of bone repair materials

Christophe Drouet *, Marie-Thérèse Carayon, Christèle Combes, Christian Rey

CIRIMAT, CNRS/INPT/UPS, ENSIACET, 118 route de Narbonne, 31077 Toulouse Cedex 04, France

Keywords:
Biomaterials
Activation
Nanocrystalline apatites
Surface exchange
Biomimetism

A B S T R A C T

The surface activation of calcium phosphate-based biomaterials for bone repair is an emerging route for improving bone regeneration processes. One way for such activation is through the exchange of surface calcium ions with biologically-active cations such as Mg^{2+} or Sr^{2+}. In this work, the interactions of non-carbonated and carbonated nanocrystalline apatites with Mg^{2+} and Sr^{2+} were investigated by means of ion exchange experiments in solution. Langmuir-type isotherms were determined. For both Sr and Mg, a greater uptake was observed on the carbonated sample, and on both types of apatites the maximum strontium uptake was greater than that of magnesium. Inverse exchanges showed that the proportion of reversibly fixed ions after surface exchange was close to 85% for Mg and 75–80% for Sr. The results are related to the presence of a surface hydrated layer on the nanocrystals and possible exchange mechanisms are discussed. Our results favor the hypothesis of hetero-ionic surface exchanges (Mg^{2+}↔Ca^{2+}, Sr^{2+}↔Ca^{2+}) within the hydrated layer, and some analogy with octacalcium phosphate (OCP) is considered. This work should prove helpful for the control and understanding of the activation of synthetic apatite-based powders or scaffolds with bioactive elements, as well as for the global understanding of biomineralization processes.

1. Introduction

Apatitic calcium phosphates are major constituents of the mineral part of hard tissues [1]. These compounds can be described by the general formula:

$$Ca_{10-(x-u)}(PO_4)_{6-x}(HPO_4, CO_3)_x(OH, F, \ldots)_{2-(x-2u)}$$

with $0 \le x \le 2$ and $0 \le 2u \le x$. One of their specificities is their great compositional flexibility, enabling to accommodate large numbers of ionic substituents and vacancies [2].

The bone mineral, especially in the case of young bones, is composed of non-stoichiometric nanocrystalline apatites. It was shown that such biological and synthetic apatites involved "non-apatitic" chemical environments, such as labile carbonate and HPO_4^{2-} ions [3,4], most probably located on a hydrated layer at the surface of the nanocrystals [5–7]. Some structural features of nanocrystalline apatites, drawn from spectroscopic data, were found to be related to dicalcium phosphate dihydrate (DCPD) and octacalcium phosphate (OCP) [8]. Interestingly, these two hydrated phases exhibit the lowest surface tensions among several calcium orthophosphates tested [9], and the presence of a hydrated layer on nanocrystalline apatites could contribute to the reduction of their surface energy [10].

Biological apatites are known to have the capacity to exchange surface ions with the surrounding fluids [11], and the surface can be considered as a reservoir for mineral ions, capable of both fixing and releasing them as needed for the accomplishment of primary biological functions. Among such ions, Mg^{2+} and Sr^{2+} are of particular interest. Indeed, magnesium is one of the most abundant foreign elements in biological hard tissues [12] and it affects their formation and overall properties [13]. Strontium, a minor constituent of bone, has been shown to play an important role in biological processes such as homeostasis and in the treatment of some pathologies [14]. Thus, Marie et al. [15] showed that strontium exhibited clear pharmacological effects on bone, including antiresorptive and anabolic activity, which indicate a potential interest for the treatment of osteoporosis and other osteopenic pathologies.

Although cationic substitutions into the apatite network have extensively been studied in the literature, very few data are available concerning ion exchanges on biomimetic calcium-deficient nanocrystalline apatites. Yet, these compounds are of primary importance in the biomedical field since they mimic bone mineral, and they exhibit numerous features that greatly differ from a stoichiometric, well-crystallized apatitic network, especially concerning the nanometer dimensions of the apatite crystals and the presence of a hydrated layer on the surface of the nanocrystals.

A preliminary work [7] showed that magnesium and strontium ions could be taken up on nanocrystalline apatites during their maturation in solution, which is related to the evolution of thermodynamically unstable non-stoichiometric apatites toward better

* Corresponding author. Tel.: +33 5 62 88 57 60; fax: +33 5 62 88 57 73.
E-mail address: christophe.drouet@ensiacet.fr (C. Drouet).

doi:10.1016/j.msec.2008.04.011

crystallized apatites, accompanied by a reduction of the extent of the surface hydrated layer on the nanocrystals [16]. Most of the magnesium taken up was then found to be reversibly fixed, independently of the maturation stage of the apatites. On the contrary, the amount of reversibly fixed Sr^{2+} ions decreased noticeably with maturation in a Sr-containing solution. These findings suggested that Mg remained mostly on the surface of nanocrystalline apatites whereas Sr was progressively incorporated into the growing apatitic domains of the nanocrystals.

In the present paper, in contrast to previous literature reports, biomimetic apatites were firstly synthesized, matured and freeze-dried, and the powders were then contacted with Mg^{2+} and Sr^{2+} ions in a second step. This sequence was selected here in order to mimic the post-treatment procedures that can be used by manufacturers for the post-activation of apatite-based materials with Mg^{2+} or Sr^{2+} ions. In this work, the interaction of such ions with nanocrystalline apatites is studied through fast ion exchange experiments and the $Ca^{2+}\rightarrow Mg^{2+}$ and $Ca^{2+}\rightarrow Sr^{2+}$ exchange isotherms are determined for a carbonated and a non-carbonated sample. The exchangeability of Mg^{2+} and Sr^{2+} ions is also investigated in order to evaluate the amount of ions potentially available for interactions with surrounding fluids in vivo.

2. Experimental

2.1. Synthesis of nanocrystalline apatites

The sample hap-1d, a non-carbonated nanocrystalline apatite, was synthesized at room temperature by double decomposition in aqueous medium of a solution of calcium nitrate ($Ca(NO_3)_2{\cdot}4H_2O$, 52.2 g in 750 ml) and a solution of ammonium hydrogenphosphate ($(NH_4)_2HPO_4$, 120 g in 1500 ml). The sample hac-1d, a carbonated nanocrystalline apatite, was obtained by a similar protocol but adding sodium hydrogencarbonate to the phosphate solution ($(NH_4)_2HPO_4$, 90 g and $NaHCO_3$, 90 g in 1500 ml). Such starting proportions, exhibiting an excess of phosphate ions, were chosen in order to remain under phosphate buffering during the whole precipitation time and allow nanocrystalline apatite formation. In this work, sodium hydrogencarbonate was preferred to the ammonium salt as the carbonate source, due to the usual presence of carbamate impurities in the latter. The sodium content of the carbonated powders was followed. The precipitates were left maturating in the mother solution for 1 day, filtered, washed with deionized water and freeze-dried.

2.2. Ion exchange experiments

Direct ion exchange experiments have been carried out at two selected temperatures, 22 °C and 37 °C, as specified in the text, by soaking the samples in a solution containing the target ion, namely Mg^{2+} or Sr^{2+}, using a constant solid-to-liquid ratio (200 mg powder in 50 ml solution). The duration of the immersion in the exchange solution was set to 12 min (2 min under stirring and 10 min static). This duration was found to be sufficient to lead to a stabilized amount of Mg^{2+} or Sr^{2+} ions fixed on the apatite crystals. Indeed, an increase of the duration of the exchange experiment between 12 min and 1 h did not lead to an increased amount of ions fixed.

For the establishment of ion exchange isotherms, the ion concentration in the exchange solution was varied in the range 0–3.5 M and equilibrated concentrations were considered. After exchange experiment, the powder was filtered, washed with deionized water and freeze-dried.

Inverse exchange experiments were performed in a similar way as above by soaking pre-exchanged samples in a solution containing Ca^{2+} ions at varying concentrations, for 12 min, and the powders were filtered, washed with deionized water and freeze-dried.

2.3. Characterization techniques

The chemical composition of the apatites synthesized was determined by complexometry for the determination of the calcium content, by spectrophotometry for the total phosphate content (sum of PO_4^{3-} and HPO_4^{2-}), and by coulometry (UIC Coulometrics) for the measure of the amount of carbonate, which is determined from the extent of CO_2 released upon treating the samples in acidic conditions. The amount of HPO_4^{2-} ions present in the sample hap-1d was determined indirectly by comparison of the data obtained by spectrophotometry [2] before and after heating the sample at 600 °C, this heating treatment leading to the conversion of HPO_4^{2-} to $P_2O_7^{4-}$, not measurable by UV–visible spectrophotometry (Hitachi U1100). Note that the determination of the HPO_4^{2-} content was not possible on the carbonated sample due to a parallel reaction between HPO_4^{2-} and carbonate species.

The crystal structure of the samples was investigated by powder X-ray diffraction using an Inel diffractometer CPS 120 and the monochromatic CoK_α radiation (λ_{Co} = 1.78892 Å). The acquisition time was set to 15 h.

The specific surface area, S_w, of the samples was determined using the BET method (nitrogen adsorption) on a Nova 1000 Quantachrome apparatus.

Fourier transform infrared (FTIR) analysis was carried out on a Perkin Elmer 1700 spectrometer with a resolution of 4 cm^{-1}, using the KBr pellet method.

The magnesium and sodium content of the samples was determined by atomic absorption (Perkin Elmer A-Analyst 300) after dissolution in perchloric acid. The strontium content was measured by ICP-MS (Perkin Elmer Elan 6000).

3. Results and discussion

3.1. Powder characterization

Synthetic non-carbonated, hap-1d, and carbonated, hac-1d, apatites were prepared in this work. Their apatitic structure was assessed by XRD. Their main physical–chemical characteristics are reported in Table 1. The Ca/(P+C) mole ratio was found to be 1.46 for hap-1d and 1.41 for hac-1d. These values, noticeably lower than 1.67, point out the high non-stoichiometry of these compounds. Also, a HPO_4^{2-} content close to 1.10 ions per unit formula $Ca_{10-(x-u)}(PO_4)_{6-x}(HPO_4)_x(OH)_{2-(x-2u)}$ was evaluated from experimental data for the sample hap-1d, which is another element indicating its non-stoichiometry. Due to the use of a sodium salt as carbonate source for the preparation of the sample hac-1d, the initial sodium content of hac-1d was also measured (0.37 wt.%).

Table 1
Chemical-physical characteristics for hap-1d and hac-1d

Sample ref.	Ca/P (mol)	Ca/(P+C) (mol)	Mean crystal size (Å)		HPO_4^{2-} (mol per unit[a])	x_{CO3} (mol per unit[a])	S_w (m^2/g)
			(002)	(310)			
hap-1d	1.46	1.46	265	60	~1.10	–	119
hac-1d	1.53	1.41	140	45	Not determined	0.46	144

[a] Formula unit: $Ca_{10-(x-u)}(PO_4)_{6-x}(HPO_4, CO_3)_x(OH)_{2-(x-2u)}$ with $0 \le x \le 2$ and $0 \le 2u \le x$.

Taking into account the presence of sodium in hac-1d leads to the "corrected" compositional ratio (Ca+Na)/(P+C)≅1.43, which is a better parameter for the evaluation of the non-stoichiometry of this compound.

Biological apatites have been shown to be composed of nanosized plate-like crystals [17]. The mean crystal dimensions were estimated here from X-ray diffraction data based on Scherer's formula applied to peaks (002) and (310) and the results (Table 1) indicate that both samples are nanocrystalline, with crystal sizes comprised between 140 and 265 Å in length and with an average between their width and depth in the range 45–60 Å.

FTIR analysis on the sample hac-1d (Fig. 1) indicated the presence of absorption bands at 1466 (broad) and 1421 cm^{-1} and in the region 850–900 cm^{-1}. In this last region, a close examination reveals the presence of three overlapped contributions, whose positions were determined by the profile analysis software as a maximum at 874 cm^{-1} and two shoulders at 878 and 867 cm^{-1} (Fig. 1). These band positions differ slightly from typical B-type carbonated apatites and show some similarities with amorphous carbonate species. This can, most probably, be related to the presence of labile carbonates on the surface of the crystals [18].

3.2. Experimental results for Mg/Ca and Sr/Ca exchanges

In order to approach a mathematical description of ion exchange isotherms, a fit to the Langmuir model was applied, which can be described by the equation:

$$N_a = N_m \cdot \frac{b \cdot C}{1 + b \cdot C} \quad (1)$$

where N_a is the amount of ions fixed (μmol/m^2 of apatite powder), N_m is the maximum exchange amount for this ions (μmol/m^2), b is the affinity constant (l/mol) of the solid and C is the concentration of the ion at equilibrium (mol/l) in the exchange solution.

The amount of magnesium fixed on the samples hap-1d and hac-1d after direct Mg^{2+}→Ca^{2+} exchange (meaning magnesium replacing calcium), at 22 °C, was determined by atomic absorption. The corresponding isotherms are plotted in Fig. 2.

In these conditions, the refined value of N_m is N_m=5.3 μmol Mg^{2+}/m^2 for hap-1d (0.63 mmol Mg^{2+}/g) and N_m=5.6 μmol Mg^{2+}/m^2 for hac-1d (0.81 mmol Mg^{2+}/g). It is interesting to note that the maximum exchange amount for magnesium is greater in the case of the carbonated apatite. The affinity constants derived from the Langmuir fit are close to 6.2 l/mol for hap-1d and 12.7 l/mol for hac-1d. Despite some scattering of experimental points, and the fact that the Langmuir model only approximates the samples behavior, these values clearly point out a greater affinity for magnesium in the case of the carbonated sample (Table 2).

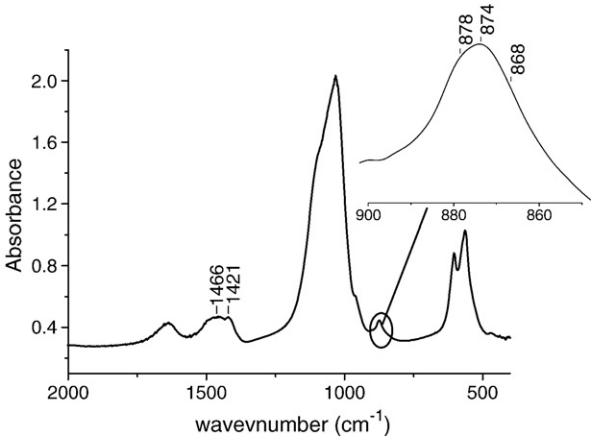

Fig. 1. FTIR spectrum of hac-1d, with positions of carbonate absorption bands.

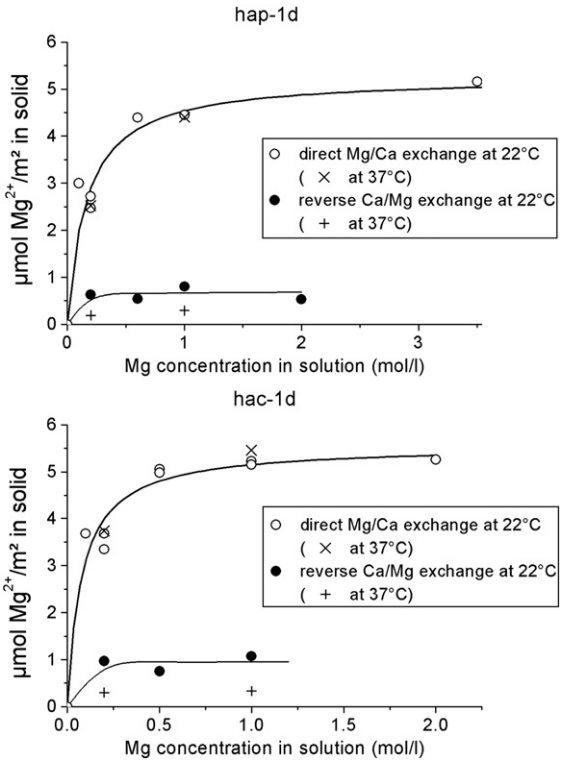

Fig. 2. Mg^{2+} uptake on hap-1d and hac-1d after direct and inverse exchange with Ca^{2+}.

Some exchange experiments were also carried out close to physiological temperature (37 °C) and the data points obtained have been added in Fig. 2. As can be seen, no significant differences were observed between the direct Mg^{2+}→Ca^{2+} exchanges obtained at 37 °C and at 22 °C.

The results obtained with the direct Sr^{2+}→Ca^{2+} exchange show general trends similar to Mg^{2+}→Ca^{2+}. The corresponding isotherms obtained at 22 °C and fitted to the Langmuir model are plotted in Fig. 3. In this case, the maximum exchange amounts are N_m=6.3 μmol Sr^{2+}/m^2 for hap-1d (0.75 mmol Sr^{2+}/g) and N_m=8.6 μmol Sr^{2+}/m^2 for hac-1d (1.24 mmol Sr^{2+}/g), with affinity constants b close to 25.0 l/mol for hap-1d and 29.1 l/mol for hac-1d. As for magnesium, the parameters N_m and b obtained for strontium are greater in the case of the carbonated sample. In addition, these N_m values show that the uptake of Sr^{2+} ions is notably greater than that of Mg^{2+}, for both kinds of apatites.

The amount of sodium present in hac-1d after ion exchange with magnesium and strontium ions, respectively, was measured. For both ions, this amount was close to 0.22 wt.% for a concentration in the exchange solution of 1 M. This value is similar to the one (0.24 wt.%) obtained after washing hac-1d in deionized water using the same washing protocol as for the exchange experiments. The comparison of these values with the initial sodium content (0.37 wt.%) indicates that in all cases part of the sodium initially present in the sample hac-1d

Table 2
Langmuir parameters for Ca^{2+}/Mg^{2+} and Ca^{2+}/Sr^{2+} exchanges on hap-1d and hac-1d

Sample	Maximum exchange amount[a], N_m (mmol/g)		Estimated affinity constant[a], b (l/mol)	
	Mg^{2+}	Sr^{2+}	Mg^{2+}	Sr^{2+}
hap-1d	0.63	0.75	6.2	25.0
hac-1d	0.81	1.24	12.7	29.1

[a] Values derived from Langmuir fit.

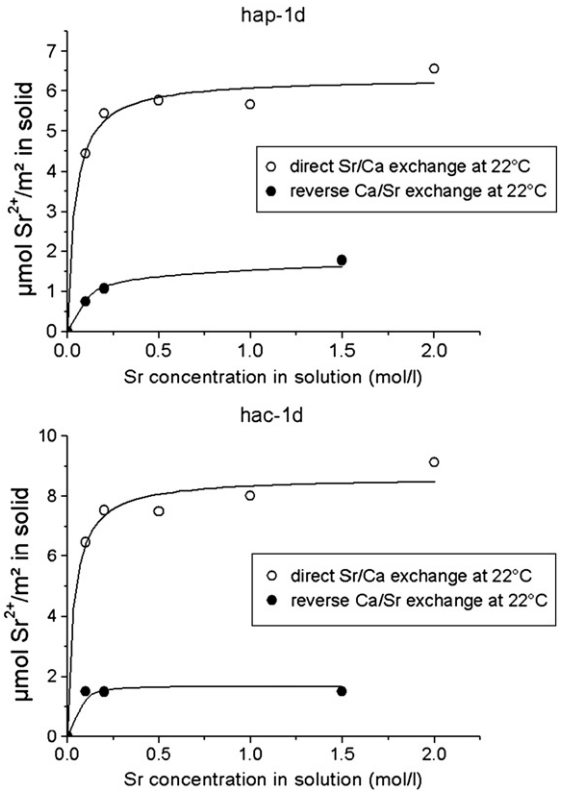

Fig. 3. Sr^{2+} uptake on hap-1d and hac-1d after direct and inverse exchange with Ca^{2+}.

was eliminated during the washing process, and no noticeable effect of the ion exchange on the sodium content of hac-1d was observed, meaning that Na^{+} ions do not participate to the calcium/magnesium or calcium/strontium exchanges.

The inverse exchanges $Ca^{2+}\rightarrow Mg^{2+}$ and $Ca^{2+}\rightarrow Sr^{2+}$ were also investigated, with the aim of determining the proportion of Mg^{2+} and Sr^{2+} ions fixed in a reversible way on the samples. After inverse exchange carried out in a calcium-rich solution, the amounts of Mg and Sr remaining in the solids hap-1d and hac-1d were measured and the comparison of the Mg and Sr contents after direct and after inverse exchange is shown in Fig. 4, for the concentration 1 M for the ion exchange solution. As can be seen, the vast majority of the Mg^{2+} and Sr^{2+} ions fixed after direct surface exchange was released during inverse exchange, as the proportions of reversible uptake were close to 85% for magnesium and 75–80% for strontium. These values are of the same order as the ones reported in an earlier study [7]. Only slight differences on this proportion were observed between hap-1d and hac-1d. For inverse exchange experiments performed at 37 °C, slightly smaller Mg contents were found to remain in the solids, pointing out an increase in magnesium exchangeability (~93%) at this temperature. This indicates that for apatites matured for one day (i.e. hap-1d and hac-1d), most of the magnesium and strontium remain exchangeable. Inverse exchange experiments carried out with varying calcium concentrations, in the range 0.2–1 M, led to similar reversible/irreversible results.

In order to follow quantitatively the effects of such ion exchange processes, ionic contents in the apatite powders were measured experimentally after direct and reverse exchanges, as well as after another Mg/Ca exchange cycle. In a typical example, Fig. 5 illustrates the calcium and magnesium contents measured in the powder hac-1d in the case of Mg/Ca/Mg exchanges. It shows that, in all cases, the total amount of ions Ca+Mg remains constant, whereas the change in Mg content incorporated in the solid after Mg/Ca exchanges coincides well with the change in Ca content.

3.3. Discussion on surface ion exchange mechanism

The experimental results reported here point out the greater ability for carbonated apatites to fix cations such as Mg^{2+} and Sr^{2+} as compared to non-carbonated samples. McClellan et al. [19] have reported a correlation between the magnesium and carbonate contents in sedimentary carbonated apatites. These authors suggested that Mg^{2+} and CO_3^{2-} substitutions could combine to enable the structure to physically compensate each other. Legeros [20] also reported that the presence of carbonate ions increased the Mg^{2+} content in hydroxyapatite precipitated from aqueous media. However, these works dealt with apatites precipitated in the simultaneous presence of magnesium and carbonate ions and not, as is the case here, with carbonated apatites enriched in magnesium by subsequent ion exchange in a Mg^{2+}-containing solution.

The results obtained from inverse ion exchange experiments indicate that the vast majority of Mg and Sr ions (except for samples maturated for extended periods of time [7]) is reversibly fixed on such apatites and can be released in a solution concentrated in Ca^{2+} ions. The reversibility of the exchanges Ca^{2+}/Mg^{2+} and Ca^{2+}/Sr^{2+} shows that Ca^{2+} ions can re-enter the sample surface, provoking the simultaneous release of Mg^{2+} or Sr^{2+} ions respectively. Moreover, it was shown in an earlier study [7] that the exchangeability of strontium decreased with the maturation of the apatite, suggesting that Sr was eventually

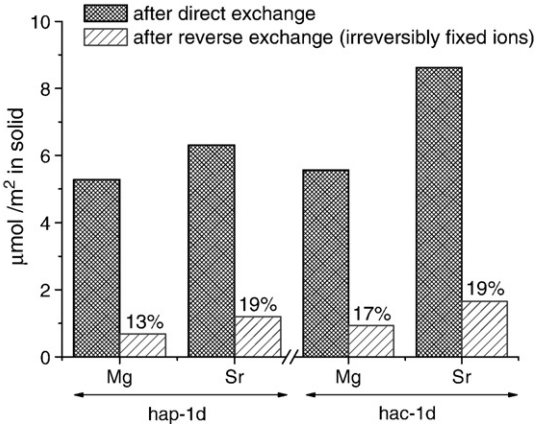

Fig. 4. Comparison of Mg and Sr contents after direct and inverse exchange, at 22 °C, on hap-1d and hac-1d (the percentages represent the proportion of irreversibly fixed ions in each case).

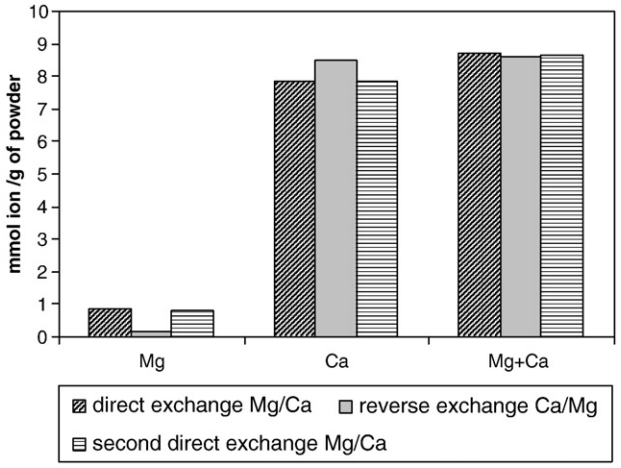

Fig. 5. Mg^{2+} and Ca^{2+} contents in hac-1d after successive direct and reverse exchange processes.

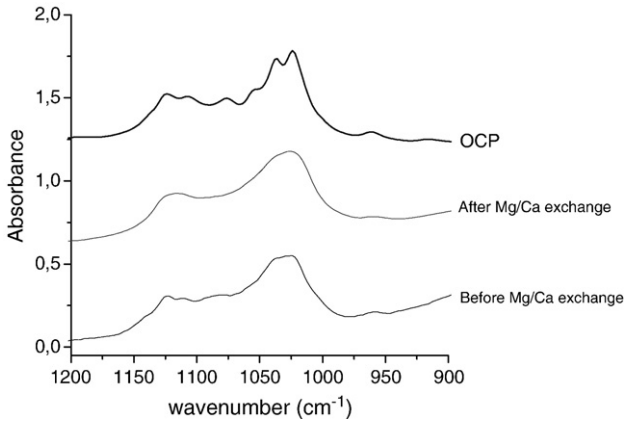

Fig. 6. Effect of Mg^{2+}/Ca^{2+} exchange on FTIR spectra ($\nu_3(PO_4)$ region) for non-matured apatites, and comparison with OCP.

included in the apatitic structure, probably in growing apatitic domains, in an irreversible way.

Based on these considerations, it is reasonable to state that the ion exchanges performed in the present work occur principally on the surface of the nanocrystals rather than in their apatitic core. This is supported by the fact that crystal size remained unchanged after ion exchange. Although the hypothesis of the formation of a secondary phase containing respectively Mg and Sr was once considered to explain Mg and Sr uptakes, it does not seem to account for all the experimental facts discussed above (high reversibility of exchange, amount of exchanging ions coinciding with change in Ca^{2+} ions, rapidity of exchange) and XRD patterns did not show the presence of other phases. In addition, it was shown [21] that rapid exchanges with magnesium or carbonate ions led to noticeable, but reversible, modifications of the hydrated layer, observable by FTIR, without changes in the long-range order (unmodified XRD patterns). Such modifications are illustrated here in Fig. 6 in the $\nu_3(PO_4)$ wavenumber region. This figure shows that numerous shoulders are clearly visible for immature apatites, and that these shoulders are highly similar to the ones observed for OCP (also reported in Fig. 6). In contrast, the figure shows that these shoulders tend to smooth out after exchange with magnesium ions. This lower resolution observed after Mg/Ca exchange indicates that the phosphate chemical environments are locally (reversibly) disturbed. Interestingly, this phenomenon was observed to be reversible.

These findings suggest that an ion exchange mechanism based on hetero-ionic substitutions between Ca^{2+} ions (from the hydrated layer of apatite nanocrystals) and Mg^{2+} or Sr^{2+} ions (from the "exchange" solution) is the most plausible interpretation. Such a mechanism is also strongly supported by the fact that the amount of ions incorporated via exchange process coincides with the amount of ions released in solution, as was shown above (see Fig. 5).

3.3.1. Effect of carbonate ions

The greater Mg and Sr uptakes (both per square meter and per gram) observed after ion exchange on the carbonated apatite sample could be related to structural differences existing between hap-1d and hac-1d, especially involving the crystals surface.

It was recently inferred that the presence of a hydrated layer on the surface of nanocrystalline apatite crystals could testify to their mode of formation in solution from isolated ions or hydrated clusters [10]. Also, carbonate ions have been shown to be growth inhibitors for the apatitic structure [22]. Therefore, if the same experimental conditions (temperature and duration of maturation in mother solution) are used to prepare a carbonated and a non-carbonated apatite, the carbonated sample is bound to be more immature, i.e. to have evolved less markedly towards a more stable apatitic phase. This difference would then lead to a greater proportion of hydrated layer as compared to the bulk, which would in turn increase the possible uptake of foreign ions through surface ion exchanges. An element illustrating this difference between carbonated and non-carbonated samples prepared in similar conditions is the lower crystallinity of the carbonated sample (Fig. 7).

3.3.2. Effect of the nature of the ion exchanged

Another important result drawn from Figs. 2 and 3 is the greater uptake observed with strontium as compared to magnesium, for both kinds of apatites.

As was mentioned above, in the case of rapid surface exchanges the Mg and Sr uptakes are bound to take place within the hydrated layer present on the nanocrystals, through hetero-ionic substitution for calcium ions. Interestingly, Aoba et al. [23] showed that Mg^{2+} and Ca^{2+} could readily replace each other at surface adsorption sites of biological and synthetic apatites. In a similar way, Fuierer et al. [24] explained the inhibitory effect of magnesium on the growth of HAP by the competitive adsorption of Ca^{2+} and Mg^{2+} at active growth sites. More recently, Ouadiay and Taitai [25] also concluded from their study on the interaction of Mg^{2+} with apatitic OCP that these ions were fixed on specific sites generally occupied by calcium.

The exact structure of this hydrated layer has not yet been determined in detail, which is partly due to its relative fragility and alteration upon drying. Some spectral features indicated however similarities between nanocrystalline apatites and OCP (triclinic) [8] which is a hydrated phase. It is interesting to remark that the structure of triclinic OCP $Ca_8(PO_4)_4(HPO_4)_2{\cdot}5H_2O$ is composed of a succession of "apatitic layers" and "hydrated layers" stacked alternatively along the (Ox) axis [26]. Within the "apatitic layers", the positions of all atoms correspond very closely to those in HAP. The alternating "hydrated layers" in OCP contain the remaining calcium ions, the HPO_4^{2-} ions and the water molecules present in the structure. It is worthwhile noting that the hydrolysis of OCP to apatite is undergone without modification of crystal morphology and that OCP has been considered as a precursor for biological apatite formation [27]. These points illustrate the strong relationship existing between OCP and apatite.

Like the alternating "hydrated layers" in OCP, the hydrated layer present on nanocrystalline apatites mostly involves bivalent ions and water, with HPO_4^{2-} ions located in non-apatitic environments [5]. Strong analogies have also been unveiled by FTIR for the $\nu_3(PO_4)$ vibration mode between OCP and apatite nanocrystals [8]. These elements suggest that, although carbonate ions have not been observed in triclinic OCP, some parallel between the interface "hydrated layer"/"apatite layer" in OCP and the interface "hydrated layer"/"apatitic core" in nanocrystalline apatites can be made (keeping in mind that in OCP a constitutive hydrated layer is surrounded by two apatitic layers, whereas in nanocrystalline apatites, the hydrated layer is present at the surface of the nanocrystals). Unfortunately, very few works have dealt with cationic substitutions or adsorption on OCP

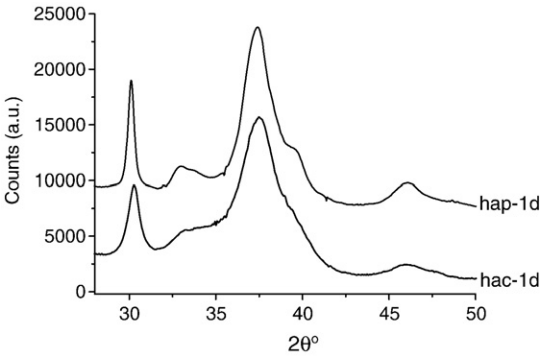

Fig. 7. XRD patterns for hap-1d and hac-1d illustrating a difference in crystallinity state.

and, to our knowledge, no discussion on site occupancies in OCP was reported. Legeros [28] reported that OCP, among other phases, could tolerate some structural imperfections and accommodate foreign ions. Also, Tung et al. [29] studied the adsorption of Mg^{2+} on synthetic OCP and showed that these ions were readily adsorbed with a Langmuir-like behavior with $N_m = 1.24$ μmol/m^2 (31.19 μmol/g with $S_w = 25.16$ m^2/g). This value is about 4.3 times lower than the one observed for magnesium uptake on hap-1d.

Among the physical–chemical parameters playing a potential role in substitution mechanisms, ionic charges and relative sizes are often major factors[2]. In the present case, the ions Ca^{2+}, Mg^{2+} and Sr^{2+} have the same +2 charge (alkali-earth). Table 3 gathers the effective ionic radii reported by Shannon [30] for Ca^{2+}, Mg^{2+}, and Sr^{2+} in six-, seven-, and nine-fold coordinations. This table shows that, generally speaking, Ca^{2+} ions are larger than Mg^{2+}, but smaller than Sr^{2+}. Therefore a consideration based solely on ion sizes of Sr^{2+} and Mg^{2+} does not seem to explain the data pointing out a greater uptake for the larger ion (Sr^{2+}).

A possible explanation for the different behaviors observed for Mg and Sr could be that these ions substitute for calcium in distinct crystallographic sites. The existence of different site preferences for Sr^{2+} and Mg^{2+} has already been discussed in the literature in the case of stoichiometric apatites, in which Sr^{2+} ions were found to preferentially occupy Ca(II) apatitic sites [31,32] whereas Elliott [2] suggested that Mg^{2+} ions most probably occupied preferentially Ca(I) "columnar" sites. In the case of surface exchanges within the hydrated layer of nanocrystalline apatites, no data are however available so far on the nature of the calcium sites.

In OCP, the calcium ions of a formula unit $Ca_8(PO_4)_4(HPO_4)_2{\cdot}5H_2O$ occupy eight distinct crystallographic sites. Fig. 8 depicts the crystallographic structure of an OCP unit cell (triclinic, space group P-1, $Z = 2$) drawn from the atomic positions and unit cell parameters given by Mathew et al. [33] and using the CaRIne Crystallography 3.1 software. The limits at $x = 1/4$ and $x = 3/4$ between hydrated layer and apatitic layer[2] have been indicated, and the eight calcium sites of a formula unit have been numbered according to earlier literature reports [34]. Among these sites, Ca1, Ca2, Ca5 and Ca8 are embedded in an apatitic layer (Fig. 8), whereas sites Ca3 and Ca4 are located within a hydrated layer. Due to their location close to the interface between hydrated layer and apatitic layer, the remaining two calcium sites Ca6 and Ca7 can probably be considered as an intermediate category of cation sites. If some parallel can be made between OCP and the surface of nanocrystalline apatites, as was discussed above, then the existence of similar categories of calcium sites probably also applies to the surface of such apatites. Although the diffusion of a substituting ion up to cation sites totally embedded in the apatitic core (like Ca1, Ca2, Ca5 and Ca8 in OCP) is presumably energetically hindered at the low temperatures involved here for the ion exchanges, the substitution in (i) calcium sites totally located in the surface hydrated layer and (ii) calcium sites in the vicinity of the interface between hydrated layer and apatitic core seems conceivable. Then, different abilities of substituting ions like Mg^{2+} and Sr^{2+} to reach these various sites could explain in part the differences in behavior observed.

However, other factors could also affect ion substitutions. From a thermodynamical point of view, the ion exchange between Me^{2+} ions

Table 3
Effective ionic radii (in Å) for Ca^{2+}, Mg^{2+}, and Sr^{2+} (Shannon, 1976)

Ion	Coordination		
	Six-fold	Seven-fold	Nine-fold
Ca^{2+}	1.00	1.06	1.18
Mg^{2+}	0.72	–	–
Sr^{2+}	1.18	1.21	1.31

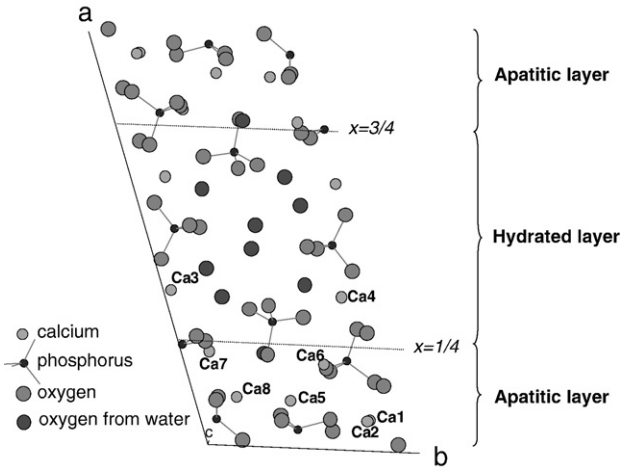

Fig. 8. Structure of triclinic OCP (hydrogen atoms were omitted for clarity).

(Me = Mg, Sr) from a solution and Ca^{2+} ions from the hydrated layer on an apatite nanocrystal can be described by the equilibrium:

$$Ca^{2+}_{\text{hydrated layer}} + Me^{2+}_{\text{solution}} \overset{K_{Me}}{\leftrightarrows} Ca^{2+}_{\text{solution}} + Me^{2+}_{\text{hydrated layer}} \quad (2)$$

where K_{Me} is the constant of the equilibrium. Although K_{Me} is not available to-date for magnesium and strontium, this constant is likely to take different values for Mg^{2+} and Sr^{2+} which exhibit different behaviors in aqueous solution. Indeed, due to the larger size of Sr^{2+} ions, the aquo complex formed with water, $[Sr(H_2O)_6]^{2+}$, is more diffuse and less energetic [35] than the complex $[Mg(H_2O)_6]^{2+}$ involving magnesium. The strong stability of the latter represents thus a potentially limiting step for the achievement of Eq. (2), where the decomposition of the complex $[Mg(H_2O)_6]^{2+}$ is required for the incorporation of free Mg^{2+} ions in cationic sites of the hydrated layer, and this could explain at least partly the greater affinity for strontium.

From the equilibrium described by Eq. (2), Le Chatelier's law indicates that the direct exchange is favored for high concentrations of exchanging cation Me^{2+} in the exchange solution, since for moderated concentrations the released Ca^{2+} ions could readily re-enter the hydrated layer. This consideration, along with the stability of the aquo complex $[Me(H_2O)_6]^{2+}$, probably explains that high concentrations (as compared to the amount of ions fixed during exchange) are required in order to observe a noticeable concentration effect.

A close analysis of the data points obtained after inverse exchanges on hap-1d and hac-1d (see Figs. 2 and 3) reveals that, for a given apatite and exchanging ion, the amount of irreversibly fixed Mg^{2+} and Sr^{2+} ions is rather constant independently of the concentration of the exchange solution used during the direct exchanges. These findings tend to point out the existence of a pre-determined capacity to host foreign cations in an irreversible way, depending only on the characteristics of the apatite and on the nature the exchanging ion. This phenomenon could be linked to the involvement of two kinds of cationic sites, as discussed above: sites located within the hydrated layer and sites situated at the interface between hydrated layer and apatitic core. The amount of irreversibly fixed ions could be linked to the incorporation of foreign cations in crystallographic sites located at the interface between the apatitic core and the hydrated layer, since these sites are presumably more likely to become part of the growing (stable) apatitic domains, whose expansion is thermodynamically-driven during maturation in solution. The invariability of the irreversible/reversible ratio for varying Ca concentrations in the inverse exchange solution goes in favor of the above hypothesis, locating such irreversibly fixed ions on crystallographic sites present at the interface between hydrated layer and apatitic core, and susceptible to irreversibly enter the stable apatitic lattice.

4. Conclusions

Aqueous ion exchange experiments involving magnesium and strontium ions were carried out on biomimetic carbonated and non-carbonated nanocrystalline apatites. For a given exchanging ion, the related isotherms showed that a greater exchange amount was reached on the carbonated sample, which was linked to a more developed surface hydrated layer than on the non-carbonated sample, probably linked to the apatite-growth inhibiting effect of CO_3^{2-} ions. In addition, a greater affinity of both kinds of apatites was found for strontium as compared to magnesium.

Possible ion exchange mechanisms were discussed, and the experimental results reported in this contribution favor the hypothesis of hetero-ionic exchanges ($Mg^{2+}\leftrightarrow Ca^{2+}$, $Sr^{2+}\leftrightarrow Ca^{2+}$) within the hydrated layer, rather than substitutions in the apatitic core or the formation of a secondary phase. This is in particular evidenced by the high reversibility of the exchanges and the nearly 1:1 substituting ratio observed. These ion exchanges might involve different site preferences among the cation sites present within the hydrated layer and at the interface between the hydrated layer and the apatitic core, which in turn could be related to the stability of $[Me(H_2O)_6]^{2+}$ (Me = Mg, Sr) complexes in solution.

These findings shed light on the interaction of biomimetic apatites with bioactive mineral ions, and should prove useful in the field of bone tissue reconstruction, in particular for the surface activation of apatite-based powders and scaffolds with ions of biological interest, as well as for the comprehension of biomineralization processes linked to the regulation of mineral ions in body fluids.

Acknowledgment

This work was supported in part by the European Commission in the scope of the AUTOBONE program (NMP Program NMP3-CT-2003-505711-1).

The authors thank S. Cazalbou, I. Pelletier and F. Bosc for technical support as well as the Laboratoire des Mécanismes et Transferts en Géologie (LMTG, UMR CNRS 5563) from Toulouse, France, where the ICP-MS analyses were performed.

References

[1] R. Legros, N. Balmain, G. Bonel, J. Chem. Res. (1986) 8.
[2] J.C. Elliott, Studies in Inorganic Chemistry, 18, Elsevier, Amsterdam, 1994.
[3] C. Rey, J. Lian, M. Grynpas, F. Shapiro, L. Zylberberg, M.J. Glimcher, Connect. Tissue Res. 21 (1989) 267.
[4] Y. Wu, J.L. Ackerman, H.M. Kim, C. Rey, A. Barroug, M.J. Glimcher, J. Bone Miner Res. 17 (2002) 472.
[5] S. Cazalbou, C. Combes, D. Eichert, C. Rey, J. Mater. Chem. 14 (2004) 2148.
[6] D. Eichert, C. Combes, C. Drouet, C. Rey, Key Eng. Mater. 284 (2005) 3.
[7] S. Cazalbou, D. Eichert, X. Ranz, C. Drouet, C. Combes, M.F. Harmand, C. Rey, J. Mater. Sci., Mater. Med. 16 (2005) 405.
[8] D. Eichert, H. Sfihi, C. Combes, C. Rey, Key Eng. Mater. 254 (2004) 927.
[9] G.H. Nancollas, W. Wu, R. Tang, Mater. Res. Soc. Symp. Proc. 599 (2000) 99.
[10] S. Cazalbou, D. Eichert, C. Drouet, C. Combes, C. Rey, C. R. Palevol 3 (2004) 563.
[11] W.F. Neuman, T.Y. Toribara, B.J. Mulryan, J. Am. Chem. Soc. 78 (1956) 4263.
[12] S. Tsuboi, H. Nakagaki, K. Ishiguro, K. Kondo, M. Mukai, C. Robinson, J.A. Weatherell, Calcif. Tissue Int. 54 (1994) 34.
[13] R.Z. Legeros, in: S. Suga, H. Nakahara (Eds.), Mechanisms and Phylogeny of Mineralization in Biological Systems, Springer-Verlag, Tokyo, 1991, p. 315.
[14] S. Pors Nielsen, Bone 35 (2004) 583 San Diego, USA.
[15] P.J. Marie, P. Ammann, G. Boivin, C. Rey, Calcif. Tissue Int. 69 (2001) 121.
[16] C. Rey, A. Hina, A. Tofighi, M.J. Glimcher, Cells Mater. 5 (1995) 345.
[17] H.M. Kim, C. Rey, M.J. Glimcher, J. Bone Miner Res. 10 (1995) 1589.
[18] C. Rey, B. Collins, T. Goehl, I.R. Dickson, M.J. Glimcher, Calcif. Tissue Int. 45 (1989) 157.
[19] G.H. McClellan, J.R. Lehr, Am. Miner. 54 (1969) 1374.
[20] R.Z. Legeros, in: R.W. Fearnhead, S. Suga (Eds.), Tooth enamel IV, Elsevier, Amsterdam, 1984, p. 32.
[21] D. Eichert, Ph.D. thesis, Toulouse, France, 2001.
[22] A.A. Campbell, M. LoRe, G.H. Nancollas, Colloids Surf. 54 (1991) 25.
[23] T. Aoba, E.C. Moreno, S. Shimoda, Calcif. Tissue Int. 51 (1992) 143.
[24] T.A. Fuierer, M. LoRe, S.A. Puckett, G.A. Nancollas, Langmuir 10 (1994) 4721.
[25] A. Ouadiay, A. Taitai, Phosphorus Sulfur Silicon 178 (2003) 2225.
[26] M. Mathew, S. Takagi, in: G.M. Whitford (Ed.), Monographs in Oral Science, 18, Karger, Basel, 2001, p. 5.
[27] W.E. Brown, Clin. Orthop. Relat. Res. 44 (1966) 205.
[28] R.Z. Legeros, in: H.M. Myers (Ed.), Monographs in Oral Science, 15, Karger, Basel, 1991, p. 11.
[29] M.S. Tung, B. Tomazic, W.E. Brown, Arch. Oral Biol. 37 (1992) 585.
[30] R.D. Shannon, Acta Crystallogr. A32 (1976) 751.
[31] V.O. Khudolozhkin, V.S. Urusov, K.I. Tobelco, Geochem. Int. 9 (1972) 827.
[32] K. Sudarsanan, R.A. Young, Acta Crystallogr. B36 (1980) 1525.
[33] M. Mathew, W.E. Brown, L.W. Schroeder, B. Dickens, J. Crystallogr. Spectrosc. Res. 18 (1988) 235.
[34] W.E. Brown, J.P. Smith, J.R. Lehr, A.W. Frazier, Nature 196 (1962) 1048.
[35] P. Pascal, Notions élémentaires de chimie générale, Masson et Cie, Paris, 1949.